Dalton Transactions

Accepted Manuscript

ROYAL SOCIETY OF CHEMISTRY

www.rsc.org/dalton

Synthesis and Characterization of Phosphorescent Platinum and Iridium Complexes with Cyclometalated Corannulene

John W. Facendola[a], Martin Seifrid[a], Jay Siegel[b], Peter I. Djurovich[a], Mark E. Thompson[a,*]

Abstract

The synthesis, structural, and photophysical characterization is reported for Pt(II) and Ir(III) complexes cyclometalated with 2-(corannulene)pyridine (corpy), (corpy)Pt(dpm) and (corpy)Ir(ppz)2 (dpm = dipivolylmethanato, ppz = 1-phenylpyrazolyl). A third compound, (phenpy)Ir(ppz)$_2$ (phenpy = 2-(5-phenanthryl)pyridyl), was also prepared to mimic the steric bulk of (corpy)Ir(ppz)$_2$. X-ray analysis reveals bowl depths of 0.895 Å for (corpy)Pt(dpm) and 0.837 Å in (corpy)Ir(ppz)$_2$. Neither complex displayed bowl-to-bowl stacking in the crystal lattice. A fluxional process for (corpy)Ir(ppz)$_2$ attributed to bowl inversion of corranulene is observed in solution with a barrier ($\Delta G^{\ddagger}$ = 13 kcal mol^{-1}) and rate (k = 2.5 x 10^3 s^{-1}) as determined using variable temperature ^{1}H NMR spectroscopy. All of the complexes display red phosphorescence at room temperature with quantum yields of 0.05 in solution and 0.2 in polymethyl methacrylate (PMMA).

Introduction

The study of fullerenes has inspired chemists to understand and probe the structural and electronic properties of these compounds as well as the applications of these molecules.[1, 2, 3, 4] Corannulene, nicknamed “buckybowl”, has been described as the smallest fullerene fragment that retains curvature.[5, 6, 7] As a result of its unique structure, corannulene has been proposed for use in many promising applications ranging from charge transport to end caps for nanotubes.[8, 9, 10]

One interesting property exhibited by corannulene as a result of its curvature is dynamic bowl-to-bowl inversion in solution. The inversion process of corannulene has been intensively studied with various substitutions, additional fused rings, as well η^2 and η^6 ligand coordinated to a transition metal. [11,12,13,14,15,16] The energy barrier to bowl inversion has been determined using variable temperature NMR, showing that substituents on corannulene control its bowl depth and thereby affect the rate of inversion.[11, 13] The rate of inversion for the parent corannulene falls within the microsecond regime, the same time scale as radiative decay for some phosphorescent heavy transition metal complexes, particularly those of iridium and platinum.[17, 18,19]

Cyclometalated iridium and platinum complexes have been studied extensively due to their efficient phosphorescence, promoted by strong intersystem crossing from the heavy metal center.[20, 21, 22, 23] The photophysical properties of these metal complexes strongly depend not only on the metal center, but also on the chemical structures of the cyclometalated (C^N) ligands. [17, 18, 24] The emission energies of such complexes are closely related to the nature of the chromophoric C^N ligand and there have been numerous in depth studies probing this relationship.[20, 25, 26]

Recently, a report has appeared of 2-(corannulene)pyridine (corpy-H) ligand precursor cyclometalated onto Pd(II).[27] Both corpy-H and a $[(corpy)Pd(ACN)_2]^+$ (ACN = acetonitrile) complex were structurally characterized and a columnar bowl-bowl packing arrangement of the corpy ligand was observed in the Pd species. In addition, a (corpy)Pd complex with an optically active ligand was also prepared; however, dynamic bowl inversion of corannulene could not be observed in this derivative. Moreover, aside from analysis of the UV-visible absorption spectrum of $[(corpy)Pd(ACN)_2]^+$, no other photophysical characterization was given for the Pd complexes.

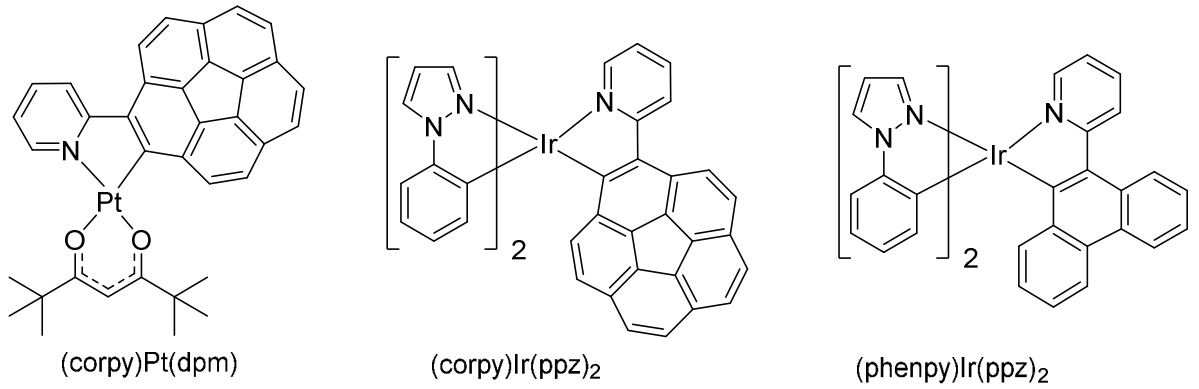

Figure 1. Structures of (corpy)Pt(dpm), (corpy)Ir(ppz)$_2$, and (phenpy)Ir(ppz)$_2$,

Herein, Pt and Ir complexes containing a cyclometalated corpy ligand are synthesized and their dynamic properties probed. The Pt complex is (corpy)Pt(dpm), where dpm = η^2-dipivolylmethane and the Ir complex is (corpy)Ir(ppz)$_2$, where ppz = 1-phenyl-1H-pyrazolyl (Figure 1). A third compound, (phenpy)Ir(ppz)$_2$ (phenpy = 2-(5-phenanthryl)pyridyl)) was also synthesized to mimic the steric bulk of (corpy)Ir(ppz)$_2$ and probe the effect of atropisomerism the dynamic behavior in solution. Variable temperature NMR is used to examine any dynamic processes that these complexes undergo in fluid solution. Both (corpy)Pt(dpm) and (corpy)Ir(ppz) are phosphorescent with the photophysical properties dictated by the corpy ligand.

Scheme 1

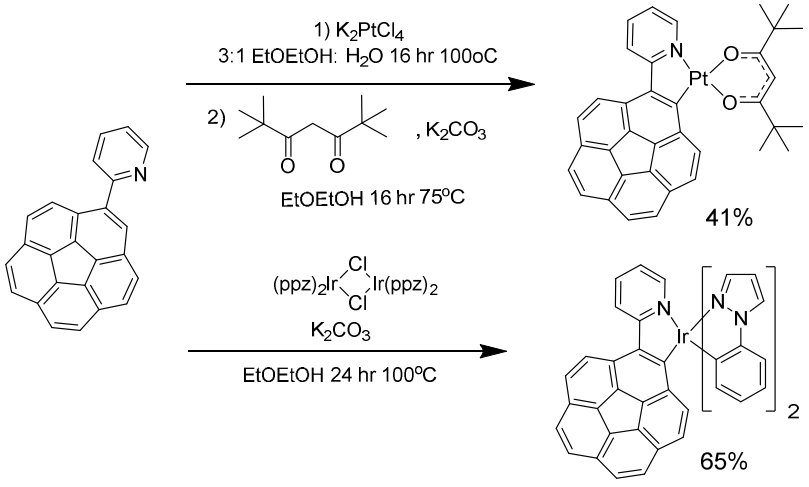

Results and Discussion

The corpy-H and phenpy-H ligand precursors were prepared by Suzuki cross coupling as described for other C^N ligands.[18] The Pt(II) and Ir(III) complexes containing corpy were prepared by routes similar to those described for other C^N complexes (Scheme 1).[17, 18,31] The (corpy)Pt(dpm) complex was synthesized by first preparing a cyclometalated (corpy)PtCl intermediate in a reaction between corpy-H and K_2PtCl_4, followed by addition of dipivalylmethane and base to displace the Cl ligand. The (corpy)Ir(ppz)$_2$ and (phenpy)Ir(ppz)$_2$ complexes were synthesized by treating the [(ppz)$_2$Ir(μ-Cl)]$_2$ dimer with the correspond ligand precursor in the presence of base. The orange colored complexes were isolated as single species that are stable in air as neat solids and in fluid solution. In addition, the Ir complexes are photolytically stable as determined by monitoring the UV-visible absorption spectra in MeCN solution before and after prolonged irradiation with 365 nm light.

Crystal Structures

X-ray diffraction analysis was performed on crystals of (corpy)Pt(dpm) and (corpy)Ir(ppz)$_2$ grown by slow diffusion of hexanes into dichloromethane of the metal complex. The structure of (corpy)Pt(dpm) is shown in Figure 2a. The unit cell of (corpy)Pt(dpm) is comprised of 8 molecules in a monoclinic C 2/c space group (Figure 2b) and contain both enantiomers of the corannulene bowl, designated P or M using the stereodescriptor system for chiral buckybowls.[28-29] The complex has a distorted square planar geometry around the metal center, with deviations from ideality due to chelate bite angles (C(1)-Pt-N(1) = 81.1(2)° and O(1)-Pt-O(2) = 89.85 (18)°) that are comparable to values found in other cyclometalated Pt(β-diketonato) complexes.[30-31] The corannulene and pyridyl fragments in the corpy ligand are

twisted with a dihedral angle of 10.6° between the two rings.

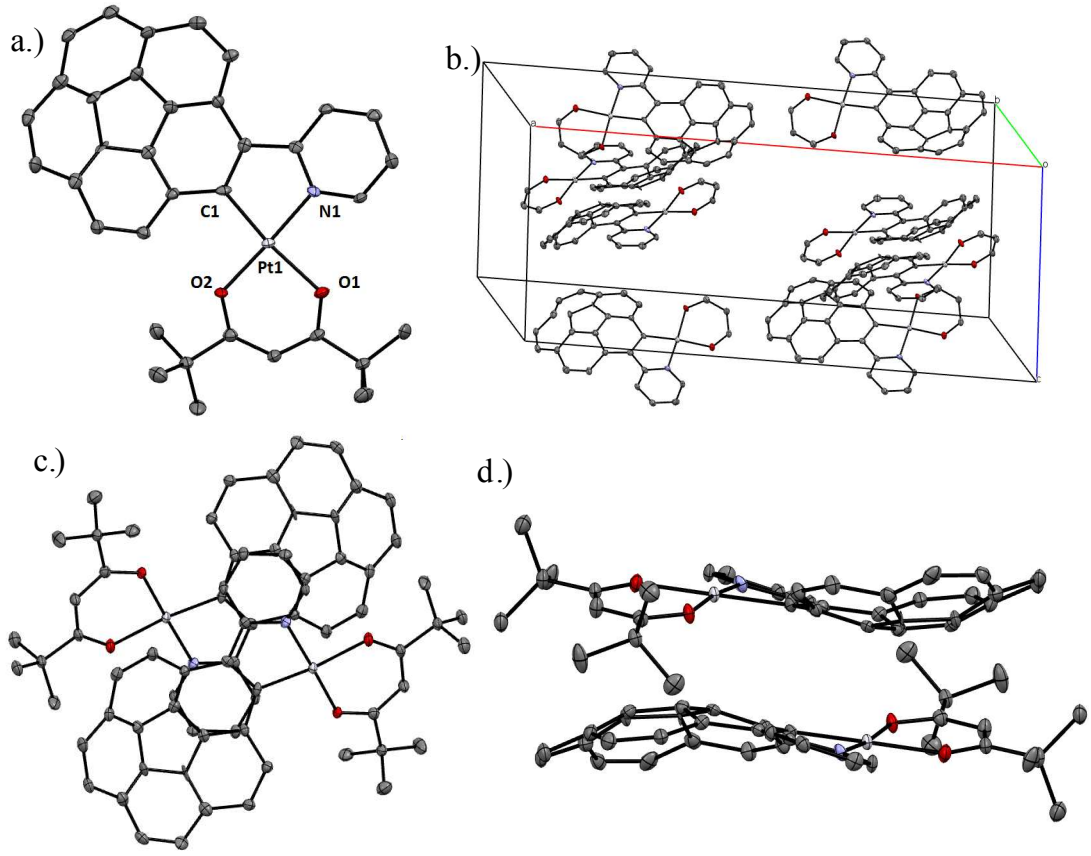

Figure 2. a.) Crystal structure of (corpy)Pt(dpm); b.) unit cell of (corpy)Pt(dpm) (methyl groups omitted for clarity); c.) top and d.) side view of (corpy)Pt(dpm) dimers. All hydrogens omitted for clarity. The atoms are colored blue (N) black (C), red (O) and gray (Pt).

There are no metal-metal interactions as the closest Pt···Pt distance is 5.65 Å. The bond lengths to the metal (Pt-C(1) = 1.984(6) Å, Pt-N(1) = 1.993(5) Å, Pt-O(1) = 2.086(4) Å and Pt-O(2) = 2.021(4) Å) are also comparable to values reported for (ppy)Pt(dpm)[20] and other Pt(β-diketonato) derivatives with cyclometalated ligands.[17, 30, 31] The bowl depth of corannulene (d_{bowl} = 0.895 Å) is similar to values in unsubstituted corannulene (d_{bowl} = 0.87 Å) and corpy-H (d_{bowl} = 0.89 Å) but deeper than found in $[(corpy)Pd(ACN)_2]^+$ (d_{bowl} = 0.82 Å).[13, 32]

Previous crystallographic studies of corannulene derivatives have shown that the molecules can preferentially π-stack in an ordered arrangement, colloquially referred to as bowl-to-bowl packing.[27, 33] For example, the $[(corpy)Pd(ACN)_2]^+$ complex is stacked in a columnar arrangement displaying corannulene-corannulene π-interactions (3.3–3.4 Å) between adjacent molecules. However, no such bowl-to-bowl stacking is present in the crystal of (corpy)Pt(dpm). Instead, complexes are arranged into antiparallel pairs of enantiomers with the convex faces of the corannulene moieties pointing towards each other (Figures 2c and d).[27, 33] The corpy ligands are situated atop one another with the closest π-interaction (~3.5 Å) between the aromatic ring of one corannulene and a pyridyl group from a neighboring molecule. [27]

The unit cell of $(corpy)Ir(ppz)_2$ contains two molecules of the complex as well as two dichloromethane solvate molecules in a triclinic $P\bar{1}$ space group (Figure 3). The ligands are arranged in a meridional (*mer*) configuration around the pseudo-octahedral metal center with the pyrazolyls in a *trans* disposed arrangement. Both enantiomers of a single diastereomer (Λ-P and

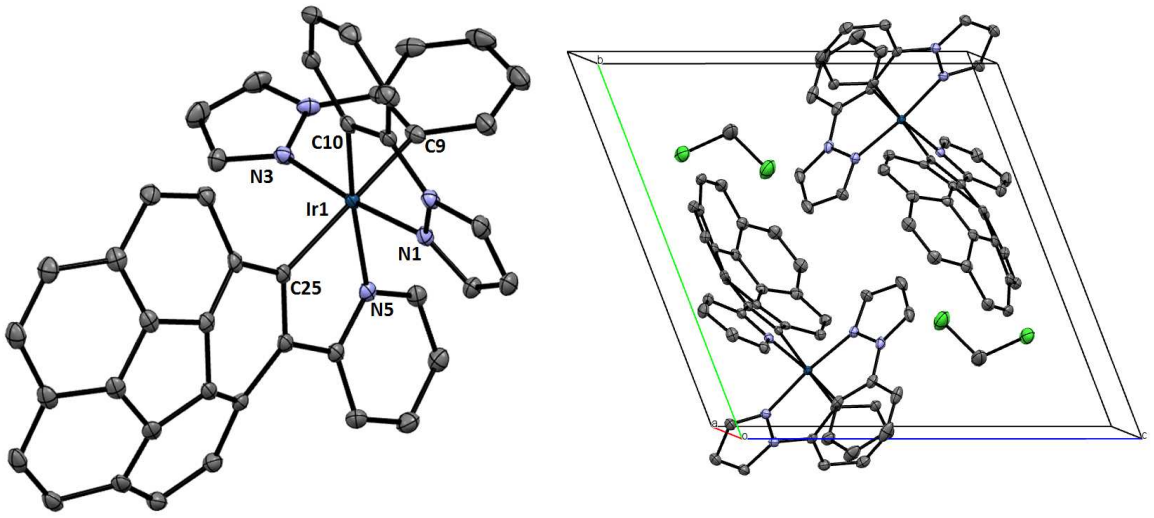

Figure 3. Crystal structure of $(corpy)Ir(ppz)_2$ (left) and unit cell (right). All hydrogens omitted for clarity. The atoms are colored by blue (N) black (C), and dark blue (Ir).

Δ-M) are present in the unit cell, where Λ and Δ describe the stereochemistry at the metal center.[28,34] The bond angles for the atoms *trans*-disposed around the metal (C(9)-Ir(1)-C(25) = 170.90(6)°, N(1)-Ir(1)-N(3) = 174.20(5)° and N(5)-Ir(1)-C(10) = 169.71(6)°) are comparable to values in other *mer*-Ir(C^N)$_3$ complexes.[18] The dihedral angle between the two fragments of the corpy ligand is 14.2°. The bond length for Ir(1)-N(5) (2.1222(13) Å) is longer than for Ir(1)-N(1) (2.0137(13) Å) and Ir(1)-N3) (2.0154(13) Å) but comparable to distances for the Ir-N(pyridyl) trans to phenyl in other *mer*-Ir(C^N)$_3$ complexes.[18] Similarly, the bond length for Ir(1)-C(25) (2.1023(15) Å) is longer than for either Ir(1)-C(9) (2.0804(16) Å) or Ir(1)-C(10) (2.0173(16) Å) bonds of the ppz ligands. The bowl depth of corannulene (d_{bowl} = 0.837 Å) is shallower than in (corpy)Pt(dpm).[13,32] No bowl-to-bowl packing is present as the corannulenyl moiety is nested with a pyrazolyl ligand from a neighboring complex.

NMR and Dynamic Behavior

The Pt and Ir complexes were characterized using ^{1}H, ^{13}C, 1D and 2D NOESY, and gCOSY NMR spectroscopy (Figure 4). Sharp, distinct resonances are observed in aromatic regions of the ^{1}H NMR spectra measured at 298 K. Peak assignments for (corpy)Pt(dpm) (Figure 4a), were made by analysis of the gCOSY spectrum. The two resonances furthest downfield are assigned to the proton **a** (δ = 9.25 ppm) adjacent to nitrogen on the pyridyl ring and proton **l** (δ = 8.92 ppm) on the corannulene ring. Both protons are deshielded due to close proximity (~2.36 Å) to the carbonyl oxygens on the dpm ligand. The remaining protons on the pyridyl ring (δ = 8.51, 7.92 and 7.14 ppm) were assigned using gCOSY. The 1D-NOESY spectrum supported assignment of the resonance at δ = 8.20 ppm to proton **e**; this proton is coupled to the remaining aromatic resonances on the corannulenyl ring located between δ = 7.70–7.85 ppm.

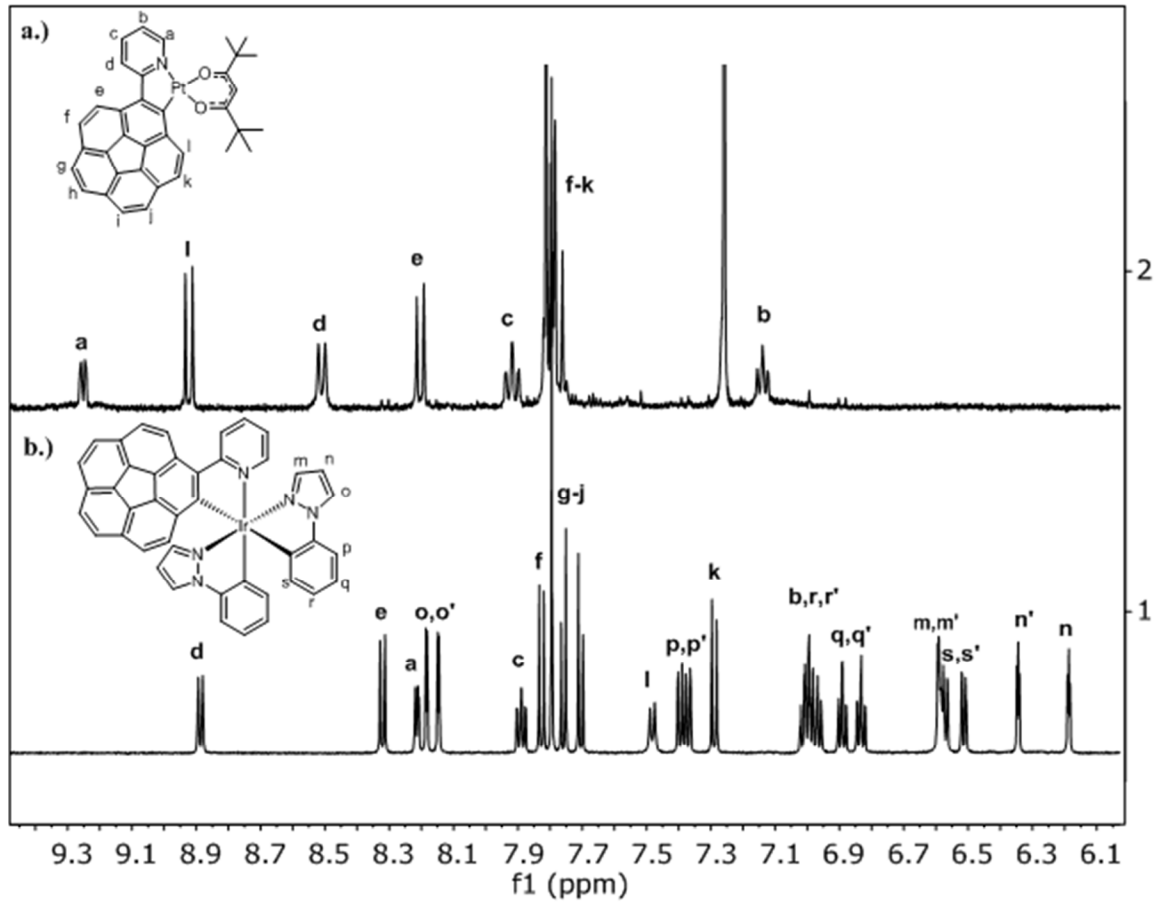

Figure 4. (a) ^{1}H NMR spectrum of (corpy)Pt(dpm) in $CDCl_3$, (b) ^{1}H NMR spectrum of (corpy)Ir(ppz)$_2$ in 2:1 CD_2Cl_2: acetone-d_6. The labelling scheme for the corpy ligand is the same in both spectra. Resonances marked with ‘ are for the ppz ligand trans to pyridyl.

The ^{1}H NMR spectrum for (corpy)Ir(ppz)$_2$ in 2:1 CD_2Cl_2:acetone-d_6 displays series of well-resolved resonances integrating to 26 protons that is consistent with a single species, even though multiple conformers are possible. The proton assignments shown in Figure 4b were confirmed on the basis of gCOSY and 1D-NOESY spectroscopy. Resonances for protons **d** (δ = 8.87 ppm) and **e** (δ = 8.32 ppm) on the corpy ligand are now the furthest downfield as protons **a** (δ = 8.22 ppm) and **l** (δ = 7.47 ppm) are shifted upfield due to shielding by the ring currents of the adjacent ppz ligands. Resonances for protons **f-j** on corranulene are distinct between δ = 7.7–7.8 ppm as

is proton **k** (δ = 7.27 ppm). The remaining protons on the pyridyl and ppz ligands are likewise clearly identified and assigned, with protons on the pyrazolyl ligands being furthest upfield (**n'**, δ = 6.34 ppm; **n**, δ = 6.19 ppm).

The (corpy)Ir(ppz)$_2$ complex undergoes a dynamic process in fluid solution that was studied using variable temperature (VT) ^{1}H NMR spectroscopy (Figure 5). A solvent mixture of 2:1 CD_2Cl_2: acetone-d_6 was used to provide good separation of all proton resonances and to maintain adequate solubility of the complex at low temperatures. Proton resonances of the corpy ligand, as well as specific resonances on the ppz ligands, broaden in stages when a sample is cooled

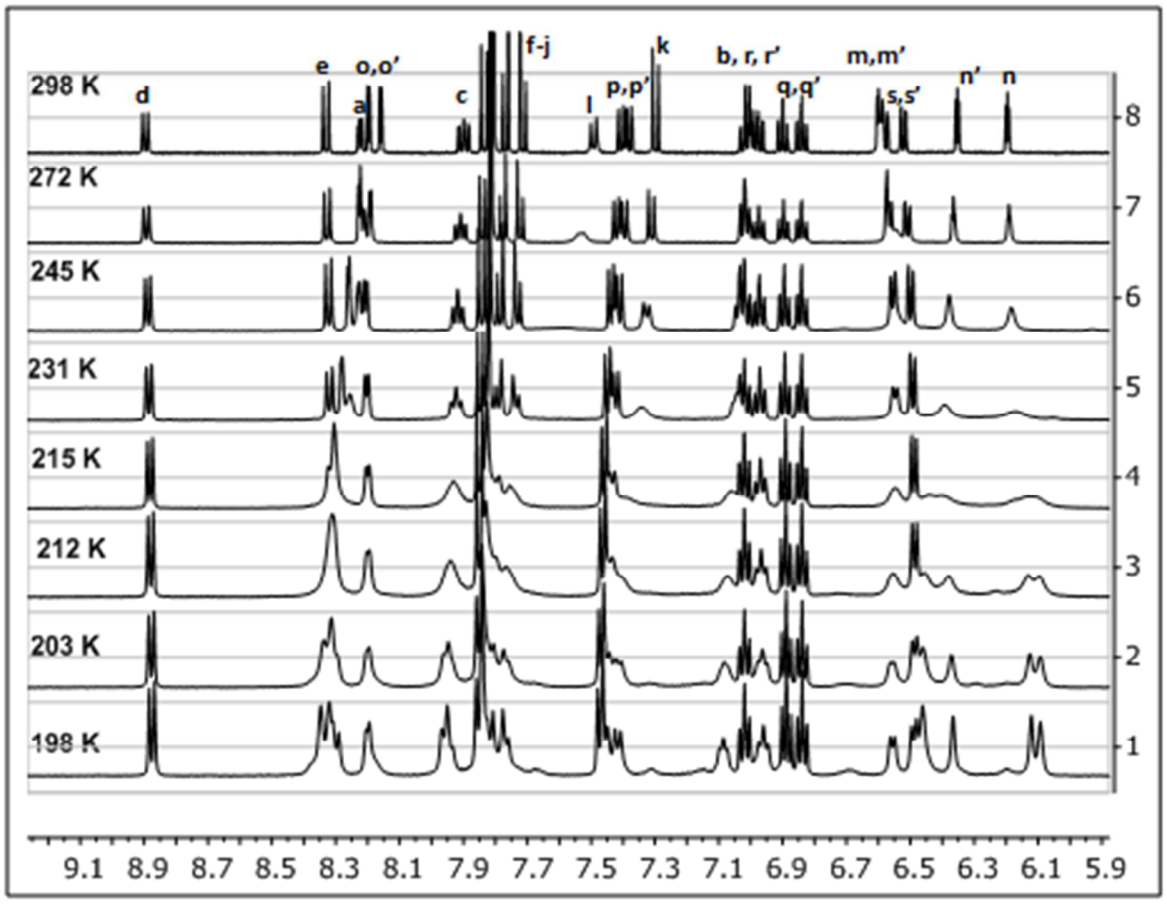

Figure 5. Variable temperature ^{1}H NMR spectra of (corpy)Ir(ppz)$_2$ in 2:1 CD_2Cl_2: acetone-d_6.

below room temperature. Initially, the resonance for proton **l** (δ = 7.47 ppm) broadens and merges into the baseline at 245 K. This change is concurrent with broadening of signals from protons **k**, **m'**, **m**, **n'** and **n** that achieve coalescence at 231 K. It is readily apparent in the spectra measured at 245 K and 231 K that signals for protons **n'** and **n** broaden at different rates. Additional broadening occurs for most of the remaining protons on corpy and the ppz ligands between 231 K and 198 K. However, some resonances, specifically from the phenyl protons **p**-**s** on ppz, and surprisingly **q'** on ppz and **d** on pyridyl, remain sharp at all temperatures. It should also be noted that weak, broad signals grow in near the baseline at the lowest temperature reached during the experiment (198 K). These new resonances, in a molar ratio of approximately 1:4.5, are tentatively assigned to a second diasteromer of (corpy)Ir(ppz)$_2$. Unfortunately, definitive identification of this new species cannot be made as we were unable to obtain clearly resolved signals due to the inability of our spectrometer to collect data to lower temperatures.

The dynamic behavior displayed by (corpy)Ir(ppz)$_2$ in the VT ^{1}H NMR spectra is consistent a bowl-to-bowl inversion process occurring on the corannulene moiety of corpy. Corannulene has an intrinsic permanent dipole moment (2.07 D) with enhanced electron density localized in the base of the bowl.[35] The dipolar flip that accompanies inversion of the bowl should strongly affect protons closest to corpy ligand. Protons that are especially useful for interpretation of the fluxional process are labeled on molecular models of the two interconverted structures shown in Figure 6. These protons (**l, m, m', n** and **n'**) have anisotropic chemical shifts that depend on the orientation of the corannulene bowl. The relation of the bowl (concave or convex) to the pyrazolyl protons will dictate whether their resonances are shielded or deshielded by the

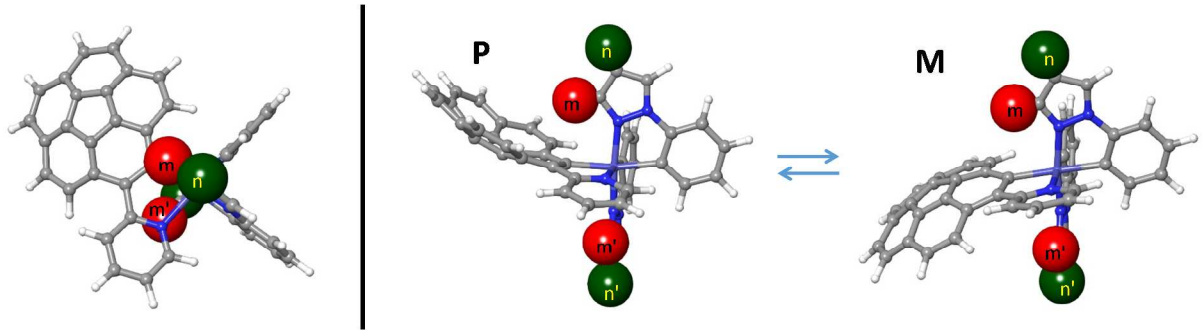

Figure 6: Structural representations of (corpy)Ir(ppz)$_2$. Protons **m** and **m'** are shown in red and **n** and **n'** in green. A view down the N–Ir–N axis is shown at the left. To the right is a view roughly down the N–Ir–C axis showing the Λ-P (left) and Λ-M (right) diastereomers of (corpy)Ir(ppz)$_2$.

direction of the dipole. The fluxional behavior is manifested as an average chemical shift at room temperature.

Kinetic analysis of the VT ^{1}H NMR spectra was carried out using the resonance at δ = 6.3 ppm assigned to the pyrazolyl proton **n** (Figures 4b and 6). The rate of inversion was determined through Eyring analysis of the line width (Δν) as a function of temperature (see Supplemental Information).[36] Values of $\Delta H^{\ddagger}$ (4.9 kcal mol^{-1}) and $\Delta S^{\ddagger}$ (-27 kcal mol^{-1}) were determined from curve fitting and the energy barrier, $\Delta G^{\ddagger}$, was found to be 13 kcal mol^{-1}, corresponding to a rate for inversion of 2.5 x 10^3 s^{-1} at room temperature. On the basis of studies on corannulenes substituted at the peri-positions, Siegel and coworkers established a correlation between the rate of inversion and bowl depth. While the substitution pattern of the cyclometalated corpy in (corpy)Ir(ppz)$_2$ is at the ortho-positions, the value determined for $\Delta G^{\ddagger}$ matches the one estimated using Siegel's data and the experimental bowl depth (d_{bowl} = 0.837 Å). The close correspondence of the present result to data from Siegel's study suggests that peri- and ortho-substitution patterns affect the stability of the corannulene in a similar manner.

Inversion of the corannulene bowl is likely not the only mechanism that can account for the fluxional behavior observed for (corpy)Ir(ppz)$_2$. Another process to consider is interconversion of conformers created by the twist between the corannulene and pyridyl groups of the corpy ligand. To investigate this possibility, the (phenpy)Ir(ppz)$_2$ complex was used to provide an (C^N)Ir(ppz)$_2$ analog that can still undergo conformational isomerism but not bowl inversion. Molecular models show that the torsion angle for the bonds labelled in red in Scheme 2 (37.7°) are comparable to values for the equivalent bonds in (corpy)Ir(ppz)$_2$ (34.1°). Likewise, the ^{1}H NMR spectrum of (phenpy)Ir(ppz)$_2$ at room temperature displays 26 resonances consistent with presence of a single species undergoing rapid interconversion on the NMR timescale. Proton resonances remain sharp at all temperatures up to 342 K in $(CD_3)_2SO$ and down to 233 K in CD_2Cl_2 (see SI), indicating that atropisomerism is rapid even at low temperature. Therefore, the dominant process responsible for the fluxional behavior observed in (corpy)Ir(ppz)$_2$ (Figure 6) is likely not due to a related atropisomerism. However, the current model assumes that a simple unimolecular inversion is the only dynamic process causing decoalescence of proton resonances in (corpy)Ir(ppz)$_2$. The fact that Eyring analysis gives a large contribution for $\Delta S^{\ddagger}$ suggests that the dynamic behavior is more complex. While bowl inversion is the primary mechanism, other secondary molecular distortions may participate in the fluxional process. Another feature to consider is how the difference between the dipole moments of diastereomers formed during bowl inversion affects the solvation of the complex. As (corpy)Ir(ppz)$_2$ undergoes inversion, not only does the stereochemistry of the corannulene bowl change but so does the orientation of the

Scheme 2.

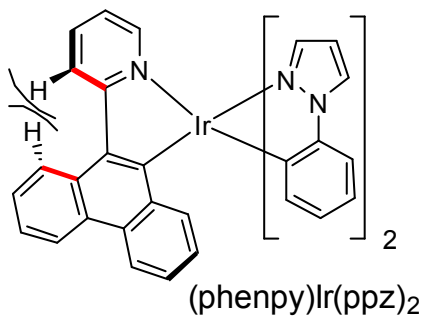

(phenpy)Ir(ppz)$_2$

dipole with respect to the $Ir(ppz)_2$ fragment. The magnitude of dipole moments calculated for the two diastereomers of $(corpy)Ir(ppz)_2$ (Λ-P = 5.27 D, Λ-M = 5.23 D) are larger than that of corannulene (2.07 D). A change in the dipole of his magnitude could cause the solvent to reorganize around the complex, leading to a large $\Delta S^{\ddagger}$ for the inversion.

Electrochemical Properties

The redox properties of the complexes were examined by cyclic voltammetry and differential pulse voltammetry in DMF solution with 0.1 M TBAF (Table 1). All potential values were referenced to an internal ferrocene couple (Fc/Fc^{+}). The oxidative properties of the complexes are similar to related derivatives with cyclometalated ligands. The (corpy)Pt(dpm) complex displays an irreversible oxidative wave at E^{pa} = 0.51 V. The potential and irreversibility of this process is comparable to oxidative behavior seen in other (C^N)Pt(dpm) complexes with expanded π-systems.[20] The Ir complexes display reversible couples at potentials ($E^{1/2}$ = 0.30 V for $(corpy)Ir(ppz)_2$ and 0.27 V for $(phenpy)Ir(ppz)_2$) that are slightly lower than *mer*-$(ppy)Ir(ppz)_2$ ($E^{1/2}$ = 0.37 V).[37] Oxidation in all of these cyclometalated complexes is typically assigned to an orbital with mixed metal-aryl character.[18,38] A second, irreversible oxidation wave is observed in the iridium complexes at higher potentials.

The complexes show reversible reduction waves in DMF solution. The (corpy)Pt(dpm) complex displays two reversible waves at -2.02 V and -2.42 V. For $(corpy)Ir(ppz)_2$ reversible reduction occurs at -2.26 V while a second quasireversible wave appears at -2.66 V. The cathodic waves in both of these complexes are assigned to reduction of the corpy ligand. These potentials are markedly less negative than the first reduction potential of $(phenpy)Ir(ppz)_2$ ($E^{1/2}$ = -2.55 V). Additional irreversible reduction waves beyond -3.0 V in the Ir complexes are

assigned to reduction of the ppz ligands. The lower potential for (corpy)Ir(ppz)$_2$ compared to (phenpy)Ir(ppz)$_2$ is consistent with the corannulene being a better electron acceptor than phenanthrene.[39,40] Similarly, the second reduction for (corpy)Pt(dpm) and (corpy)Ir(ppz)$_2$ are assigned to corpy since corannulene has been shown to undergo up to three reductions in solution.[24, 39, 41] The 400 mV separation between the first and second reduction waves in the Pt and Ir complexes is smaller than that found in corrannulene (700 mV). The difference in the metal complexes indicates a decrease in coulombic repulsion in the radical anion due to the electron being delocalized onto the pyridyl ring of the corpy ligand.

Table 1. Redox data for the Pt and Ir complexes.[a]

Compound	E_{ox1}	E_{red1}	E_{red2}	E_{red3}
(corpy)Pt(dpm)	0.51 V[b]	-2.06 V	-2.46 V	--
(corpy)Ir(ppz)$_2$	0.30 V	-2.27 V	-2.66 V[c]	-3.13 V[b]
(phenpy)Ir(ppz)$_2$	0.27 V	-2.55 V	-3.04 V[b]	--

[a]Redox potentials were recorded in 0.1 M TBAF/DMF solution and referenced to an internal Fc^+/Fc couple. [b]Irreversible. [c]Quasireversible.

Photophysical Properties

The absorption and emission spectra of the complexes were recorded at room temperature and 77 K as well as in a rigid PMMA matrix at room temperature (Figure 7). The absorption data is listed in Table 2 and emission data in Table 3. The absorption spectra for the complexes show intense bands ($\lambda < 360$ nm, $\varepsilon > 10^4$ $M^{-1}cm^{-1}$) assigned to the ligand centered $\pi\rightarrow\pi^*$ transitions on the cyclometalated ligands. In particular, the bands between λ = 300–360 nm are assigned to $\pi\rightarrow\pi^*$ transition on corpy on the basis of comparison with spectra from the free corpy-H ligand.

Less intense bands at lower energy (λ = 350–500 nm, $\varepsilon \approx 5 \times 10^3$ $M^{-1}cm^{-1}$) are assigned to allowed metal-to-ligand charge transfer (MLCT) transitions. Much weaker absorptions (λ > 500 nm, $\varepsilon < 10^2$ $M^{-1}cm^{-1}$) are assigned to triplet MLCT transitions that are partially allowed due to spin-orbit coupling with the singlet states by the heavy atom metal center.

Table 2. Absorption data for the the Pt and Ir complexes **1**–**3**.

	λ_{max}(nm) (ε, 10^3 M^{-1} cm^{-1})
(corpy)Pt(dpm) (**1**)	302 (44.8), 331 (33.8), 387 (7.90), 441 (5.82), 465 (5.76)
(corpy)Ir(ppz)$_2$ (**2**)	299 (51.4), 339 (30.2), 425 (5.93), 469 (sh, 3.00)
(phenpy)Ir(ppz)$_2$ (**3**)	300 (34.3), 403 (6.15), 450 (sh, 3.44)

[a] Absorption spectra recorded in CH_2Cl_2.

All three complexes display broad, featureless red luminescence at room temperature in 2-MeTHF solution. At 77 K, the spectra of (corpy)Pt(dpm) and (corpy)Ir(ppz)$_2$ shows distinct vibronic structure, whereas emission from (phenpy)Ir(ppz)$_2$ remains broad and relatively featureless. The emission lifetimes at 77 K are single exponential and fall in the range τ = 9.4–15 μs consistent with phosphorescence. The vibronic structure displayed by the corpy complexes indicate that emission originates from a triplet state with significant ^{3}LC character. However, the energy of the triplet state in these complexes is over 0.2 eV lower than that of the $^3\pi$-π state in the free ligand corpy-H ($E_{0\text{-}0}$ = 525 nm, 2.36 eV). The decrease in energy shows that a substantial stabilization of the excited state occurs upon cyclometalation of the ligand. Since the emission lifetimes of (phenpy)Ir(ppz)$_2$ and (corpy)Ir(ppz)$_2$ are comparable, as are the energies of the $^3\pi$-π states in the free ligands (see SI), the absence of distinct vibronic features in the former complex is likely due significant distortion in the excited state, as opposed to there being greater MLCT character in (phenpy)Ir(ppz)$_2$ than in (corpy)Ir(ppz)$_2$.

The photoluminescent quantum yields of the complexes in fluid solution are relatively low (Φ = 0.02-0.09). The radiative decay rate constants (k_r = 1.1–1.9 x 10^4 s^{-1}) are roughly an order of magnitude lower than values reported for highly efficient red Pt and Ir phosphors with cyclometalated ligands.[42,17] and indicates that the excited state has significant ^{3}LC character. However, the low quantum efficiency is mainly a consequence of rapid non-radiative decay (k_{nr} > 2 x 10^5 s^{-1}). These rates are nearly two orders of magnitude greater than what is found in efficient cyclometalated phosphors.[18] The luminescent spectra blue-shift upon dispersing the complexes in rigid media (polymethylmethacrylate, PMMA) and display vibronic features comparable to spectra recorded at 77 K. The quantum efficiencies also increase to Φ = 0.20–0.32. The higher efficiency in PMMA is mainly due to a two to four-fold decrease in k_{nr} from values measured in fluid solution. The ridigochromic shifts and decrease in non-

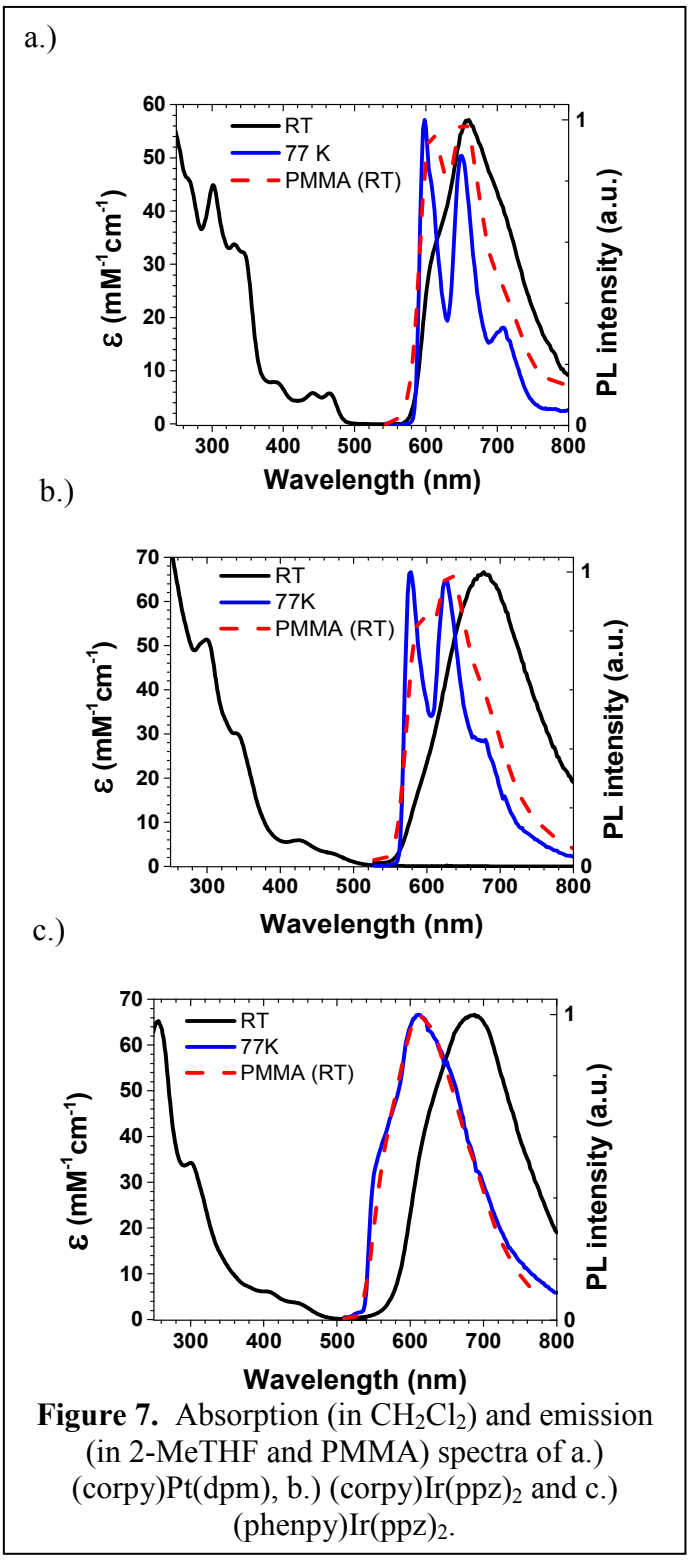

Figure 7. Absorption (in CH_2Cl_2) and emission (in 2-MeTHF and PMMA) spectra of a.) (corpy)Pt(dpm), b.) (corpy)Ir(ppz)$_2$ and c.) (phenpy)Ir(ppz)$_2$.

radiative rate constants indicate that large structural changes present in the excited state are suppressed in the rigid PMMA media. The fact that the emission lifetimes in PMMA at room temperature are comparable to values measured in 2-MeTHF at 77 K implies that vibrational deactivation remains the principal mechanism for non-radiative decay at low temperature (weak coupling limit).[43, 44, 45]

Table 3. Photoluminescence (PL) data for the Pt and Ir complexes **1**–**3**.

	solution[a]					PMMA (1% doped)			
	298 K	τ^c			77 K	298 K	τ^c	k_r	k_{nr}
	λ_{max} (nm) [Φ][b]	(μs)	k_r^d 10^4 s^{-1}	k_{nr}^e 10^4 s^{-1}	$\lambda_{0\text{-}0}$ (nm) [τ (μs)][c]	λ_{max} (nm) [Φ][b]	(μs)	10^4 s^{-1}	10^4 s^{-1}
1	660 [0.05]	5.1	1.0 ± 0.2	19 ± 3	592 [14.1]	654 [0.20]	12.0	1.7 ± 0.2	6.7 ± 1.5
2	678 [0.02]	1.7[f]	1.2 ± 0.2	58 ± 8	582 [9.4]	632 [0.20]	3.3 (14%), 8.2 (86%)	--	--
3	668 [0.09]	4.8	1.9 ± 0.3	19 ± 3	580 [15.0]	612 [0.32]	15	2.1 ± 0.3	4.5 ± 0.7

[a] Emission spectra recorded in 2-MeTHF. [b] Photoluminescent quantum yield. Error is ± 10%.[c] Error is ± 5%. [d]Derived using $\Phi = k_r\tau$. [e]Derived using $\Phi = k_r/(k_r + k_{nr})$. [f]Measured at 800 nm. See text.

An additional feature observed in the luminescent spectrum of (corpy)Ir(ppz)$_2$ is that the emission lifetime is wavelength dependent. The emission lifetime is distinctly non-first order for wavelengths <700 nm in spectra measured at room temperature with a longer decaying component appearing at higher energy. Spectra measured at 650 nm can be fit to a biexponential decay with lifetime values of τ =1.6 μs (64%), 9.4 μs (36%) in 2-MeTHF and τ = 3.3 μs (14%), 8.2 μs (86%) in PMMA. In contrast, the emission lifetimes for the other two complexes remain first-order for all wavelengths under the same conditions. The lifetime data suggests that two or more different states are emitting for (corpy)Ir(ppz)$_2$. The presence of a *fac*-isomer impurity can be excluded since no evidence of photoisomerization is observed in the UV-visible spectrum of

the complex after photolysis in acetonitrile for 8 hours with 254 nm light. The dynamic process observed in the ^{1}H NMR spectra for (corpy)Ir(ppz)$_2$ (Figure 5) gives credence for presence of two or more different species in solution, which could lead to the non-first order decay. Note that the exchange rate found by VT ^{1}H NMR at room temperature ($k_{exchange}$ = 2.5 x 10^3 s^{-1}) is much slower than either emission decay rate (k = 6.1 and 1.1 x 10^{-5} s^{-1}). Therefore, any diastereomers that form by bowl inversion are not expected to interconvert during the lifetime of the excited state and will thus emit independently. The (corpy)Pt(dpm) complex cannot show this behavior since the bowl inversion does not lead to diastereomers, but instead to enantiomers that will decay from excited states with identical rates. The fact that excited state decay from the (phenpy)Ir(ppz)$_2$ complex is wavelength independent indicates atropisomerism is not the principal cause of non-first order decay seen from (corpy)Ir(ppz)$_2$.

A possible origin for the biexponential emission decay of (corpy)Ir(ppz)$_2$ could be related to the different ligand-orbital overlaps expected in the two diastereomers, Figure 6. The excited states of organometallic Ir and Pt complexes are typically described as being mixtures of MLCT, LC and LLCT excited states (LLCT = ligand-to-ligand charge transfer).[46] Significant spectral changes in the from both of the Pt and Ir complexes with corpy ligands are seen on comparing room temperature and 77K luminescence (Figure 7), involving substantial sharpening and blue shifting on cooling. These spectral changes have been termed rigidochromism[47] and are due to changes in the ratios of MLCT:LC:LLCT, favoring LC states at low temperatures for the complexes reported here. This change suggests that mixing between the two electronic configurations is sensitive to the solvation environment around the complexes. The emission lifetime is effected by the MLCT:LC:LLCT ratio, with greater MLCT character generally giving faster radiative rates.[22] We have modeled the excited state properties of the two diastereomers of

(corpy)Ir(ppz)$_2$ using time-dependent density functional theory (TD-DFT). The complexes show the S_0-T_1 transitions for the two isomers are comprised of different amounts MLCT, LC and LLCT character, with the transition for the Λ-P isomer being 74% MLCT and that of the Λ-M isomer being 85% MLCT (see SI). Thus, since the S_0-T_1 transitions of the two isomers have different compositions it is not unreasonable to assume that the two diastereomers of (corpy)Ir(ppz)$_2$ will have unequal radiative rates, as observed. For comparison, the S_0-T_1 transition for (corpy)Pt(dpm) has > 91% MLCT character.

Conclusion

In summary, corannulene was cyclometalated onto platinum and iridium using a pendant pyridyl group to yield phosphorescent complexes. No bowl-to-bowl stacking was seen in the crystal structures of either complex. A dynamic exchange process found for (corpy)Ir(ppz)$_2$ examined using VT NMR and determined to have a rate of 2.5 x 10^3 s^{-1}. This process was modeled as an inversion of the corannulene bowl creating distinct diastereomers that rapidly interconvert at room temperature. The photophysics of the two compounds show that (corpy)Pt(dpm) and (corpy)Ir(ppz)$_2$ have large non-radiative rates at room temperature in solution, which decrease as the rigidity of the surrounding solvent increases. Additionally, the decay behavior of (corpy)Ir(ppz)$_2$ was non first-order at room temperature, differing from (corpy)Pt(dpm) as well as other common iridium phosphors. The absence of such irregular behavior in the decay from the (corpy)Pt(dpm) suggests that interconversion between diastereomers in (corpy)Ir(ppz)$_2$ is responsible for the unusual luminescent decay.

Future work will focus on dissecting the dynamics of the fluxional behavior observed in fluid solution. One such approach will be to change the identity of the pendant coordinating ligand

with a larger, bulkier heterocycle such as a quinoline or benzoimidazole to hinder any atropisomerism between the two ligand fragments. Another approach will be to alter the ancillary phenyl pyrazole ligands, using bulky substituents in order to perturb the bowl inversion process. The inherent luminescent properties of these complexes will provide an additional spectroscopic window to help elucidate the nature of this dynamic phenomenon.

Experimental

Synthesis. Chemicals were received from commercial sources and used as received. All procedures were carried out in inert N_2 gas atmosphere despite the air stability of the complexes, the main concern being the oxidative and thermal stability of intermediates at the high temperatures of the reactions. The $[(ppz)_2IrCl]_2$ dimer was synthesized by the Nonoyama method which involves heating $IrCl_3 \cdot H_2O$ to 110 °C with 2−2.5 equivalents of ppz-H in a 3:1 mixture of 2-ethoxyethanol and deionized water.[48] Corannulene was prepared as described previously.[49] The corpy-H and phenpy-H ligand precursors were prepared by Suzuki cross coupling of their respective bromo derivatives as previously described.[27,50]

(corpy)Pt(dpm). A 3 neck flask was charged with corpy-H (142 mg, 0.43 mmol), potassium tetrachloroplatinate(II) (75 mg, 0.18 mmol) and 18 mL of a 3:1 mixture of 2-ethoxyethanol:water. A condenser was attached to the flask and the mixture was degassed and heated to 100 ^{o}C for 16 hrs. The reaction was cooled to ambient temperature, then water was added to the mixture and filtered and an orange-yellow precipitate was isolated. This solid was then added to a new 3 neck flask, and then charged potassium carbonate (124 mg, 0.89 mmol) and charged with 2-ethoxyethanol. A condenser was attached and the mixture was degassed after which 2,2,6,6-tetramethylheptane-3,5-dione (56 μL, 0.27 mmol) was added and the reaction was

heated to 75°C for 16 hr. The reaction was then cooled to ambient temperature and filtered and the precipitate was then washed with methanol to give an orange emissive solid (52 mg, 41%). ^{1}H NMR (400 MHz, $CDCl_3$, δ) 1.33 (s, 7H), 1.43 (s, 7H) 5.99 (s, 1H) 7.14 (dd, *J* = 7.44, 6.07 Hz, 1H), 7.79 (m, 5H), 7.92 (dd, *J* = 8.86, 7.45 Hz, 1H), 8.20 (d, *J* = 9.00 Hz, 1H), 8.51 (d, *J* = 8.31 Hz, 1H), 8.92 (d, *J* = 8.97 Hz, 1H), 9.25 (dd, *J* = 6.09 Hz, 1H). ^{13}C NMR (101 MHz, $CDCl_3$ δ) 194.40, 169.26, 147.10, 138.28, 135.91, 135.83, 134.41, 131.68, 131.30, 130.74, 129.31, 127.94, 127.14, 126.39, 126.30, 125.41, 123.55, 121.46, 119.62, 93.64, 41.80, 41.43, 29.03, 28.39, 26.14. Anal. for (corpy)Pt(dpm): found: C 61.08, H 4.58, N 1.98; calcd: C 61.36, H 4.43, N 1.99.

(corpy)Ir(ppz)$_2$. A 3 neck flask was charged with corpy-H (65 mg, 0.20 mmol), [$(ppz)_2Ir(\mu\text{-}Cl)_2Ir(ppz)_2$] (100 mg, 0.1 mmol), potassium carbonate (116 mg, 0.84 mmol) and 12 mL of 2-ethoxyethanol. A condenser was attached to the flask and the reaction was degassed and then heated to 100 °C for 24 hrs. The reaction mixture was then cooled to ambient temperature and 10 mL of deionized water was added to dissolve excess potassium carbonate. The orange-red solid was vacuum filtered and washed with 10 mL of methanol and 10 mL hexanes, and then air dried. Column chromatography on silica gel was performed on the resultant crude mixture (100% methylene chloride) to give an orange-red emissive solid (36 mg, 65%). ^{1}H NMR (400 MHz, acetone-d_6, δ) 6.30 (dd, *J* = 3.01, 2.10 Hz, 1H), 6.43 (dd, *J* = 2.88, 2.36 Hz, 1H), 6.52 (dd, *J* = 7.56, 1.46 Hz, 1H), 6.57 (m, 2H), 6.68 (dd, *J* = 2.49, 0.71, 1H), 6.80 (ddd, *J* = 7.97, 7.42, 1.09 Hz, 1H), 6.87 (ddd, *J* = 8.01, 7.24, 1.13 Hz, 1H), 6.94 (ddd, *J* = 8.34, 7.46, 1.35 Hz, 1H), 6.99 (ddd, *J* = 8.12, 7.57, 1.67 Hz, 1H), 7.13 (ddd, *J* = 8.24, 6.77, 1.29 Hz 1H), 7.32 (d, *J* = 8.66 Hz, 1H), 7.51 (dd, *J* = 7.97, 1.32 Hz, 1H), 7.56 (m, 2H), 7.78 (d, *J* = 8.67 Hz 1H), 7.84 (d, *J* = 8.70 Hz, 1H), 7.89 (m, 3H), 8.03 (ddd, *J* = 8.19,7.72, 1.83 Hz, 1H), 8.26 (dd, *J* = 5.38,

1.73 Hz, 1H), 8.43 (m, 2H), 8.49 (dd, *J* = 2.88, 0.63 Hz, 1H), 8.99 (d, *J* = 8.20 Hz, 1H). ^{13}C NMR (101 MHz, $CDCl_3$ δ) 185.45, 169.15, 154.49, 151.82, 150.01, 143.31, 142.89, 142.36, 142.24, 141.91, 141.42, 140.35, 136.68, 136.59, 136.57, 135.29, 134.62, 134.14, 133.76, 133.01, 132.53, 131.03, 130.46, 130.43, 129.15, 128.88, 127.57, 127.37, 127.32, 127.25, 127.23, 127.21, 127.17, 127.10, 126.92, 126.87, 126.73, 126.38, 126.09, 125.96, 125.78, 125.69, 125.19, 125.17, 125.03, 124.54, 124.11, 122.98, 122.29, 121.81, 121.75, 120.62, 119.91, 110.78, 110.75, 110.39, 107.19, 106.66, 106.31. Anal. for (corpy)Ir(ppz)$_2$: found: C 63.62, H 3.31, N 8.49; calcd: C 64.16, H 3.26, N 8.7.

(phenpy)Ir(ppz)$_2$. A 3 neck flask was charged with phenpy-H (105 mg, 0.41 mmol), [(ppz)$_2$Ir(μ-Cl)$_2$Ir(ppz)$_2$] (200 mg, 0.2 mmol), potassium carbonate (215 mg, 1.56 mmol) and 26 mL of dichloroethane. A condenser was attached to the flask and the reaction was degassed and then heated to 100^{o}C for 24 hrs. The reaction mixture was then cooled to ambient temperature and filtered through an alumina plug. The resultant mixture was then recrystallized with dichloromethane to obtain yellow-orange emissive solid (58 mg, 20 %). ^{1}H NMR (400 MHz, CD_2Cl_2, δ) 6.29 (dd, *J* = 3.05, 2.54 Hz, 1H), 6.34 (dd, *J* = 7.29, 1.30 Hz, 1H), 6.40 (dd, *J* = 3.07, 2.47 Hz, 1H), 6.53 (dd, *J* = 7.20, 1.36 Hz, 1H), 6.73 (dd, *J* = 9.27, 2.30 Hz, 2H) 6.78 (ddd, *J* = 8.68,7.58, 1.10 Hz, 1H), 6.94 (m, 1H), 7.05 (ddd, *J* = 8.39, 7.55, 1.41 Hz, 1H), 7.29 (d, *J* = 7.83 Hz, 1H), 7.34 (d, 7.88 Hz, 1H), 7.42 (ddd, *J* = 8.35, 7.60, 1.15 Hz, 1H), 7.54 (m, 2H), 7.71 (ddd, *J* = 8.87, 7.89, 1.75 Hz, 1H), 8.02 (d, *J* = 8.69 Hz, 1H), 8.06 (dd, *J* = 6.20, 2.74 Hz, 2H), 8.28 (m, 2H), 8.50 (d, *J* = 8.24 Hz, 1H), 8.54 (d, *J* = 8.24 Hz, 1H), 8.67 (d, *J* = 8.36 Hz, 1H). ^{13}C NMR (101 MHz, $CDCl_3$, δ) 149.55, 142.88, 140.35, 132.53, 128.99, 128.44, 127.37, 127.03, 126.81, 126.77, 126.71, 126.56, 126.47, 125.78, 125.20, 122.72, 122.54, 121.75, 110.39, 106.31. Anal. for (phenpy)Ir(ppz)$_2$+H_2O: found: C 59.66, H 3.57, N 9.15; calcd: C 59.18, H 3.76, N 9.33.

Electrochemisty. Cyclic voltammetry and differential pulsed voltammetry were performed using an VersaSTAT 3 potentiostat. Anhydrous DMF (Aldrich) was used as the solvent under inert atmosphere, and 0.1 M tetra(*n*-butyl)ammonium hexafluorophosphate (TBAF) was used as the supporting electrolyte. A glassy carbon rod was used as the working electrode, a platinum wire was used as the counter electrode, and a silver wire was used as a pseudoreference electrode. The redox potentials are based on values measured from differential pulsed voltammetry and are reported relative to a ferrocene/ferrocenium (Cp_2Fe/Cp_2Fe^+) redox couple used as an internal reference,[51] while electrochemical reversibility was determined using cyclic voltammetry.

NMR Measurements. ^{1}H NMR spectra were recorded on a Varian-500 and a Varian 400 NMR spectrometer. Chemical shift data for each signal are reported in ppm and measured in deuterated dichloromethane (CD_2Cl_2), deuterated chloroform ($CDCl_3$), and deuterated acetone ($(CD_3)_2CO$). Variable temperature NMR was measured in the range of 198-298 K. The temperature of the NMR probe was calculated using a methanol temperature standard. The rate of inversion and inversion barrier were determined by fitting the resultant data to an Eyring plot of $\ln(kh/k_bT)$ vs $1/T$.[36]

X-ray Crystallography. The single-crystal X-ray diffraction data for compounds (corpy)Pt(dpm) and (corpy)Ir$(ppz)_2$ were collected on a Bruker SMART APEX DUO three-circle platform diffractometer with the χ axis fixed at 54.745° and using Mo Kα radiation (λ = 0.710 73 Å) monochromated by a TRIUMPH curved-crystal monochromator. The crystals were mounted in Cryo-Loops using Paratone oil. Data were corrected for absorption effects using the multiscan method (SADABS). The structures were solved by direct methods and refined on F^2 using the Bruker SHELXTL software package. All non-hydrogen atoms were refined anisotropically.

Photophysical Measurements. Photoluminescence spectra were measured using a QuantaMaster Photon Technology International phosphorescence/fluorescence spectrofluorometer. Phosphorescent lifetimes were measured by time-correlated single-photon counting using an IBH Fluorocube instrument equipped with an LED excitation source. Quantum yield measurements were carried out using a Hamamatsu C9920 system equipped with a xenon lamp, calibrated integrating sphere and model C10027 photonic multi-channel analyzer (PMA). UV−vis spectra were recorded on a Hewlett-Packard 4853 diode array spectrometer. Samples for transient luminescent decay measurements were prepared in 2-MeTHF solution. The samples were deaerated by extensive sparging with N_2.

Computational Methods. Molecular models were created and dipole moments determined using the Jaguar 8.4 (release 17) software package on the Schrodinger Material Science Suite (v2014-2). The molecular geometries and TD-DFT calculations were performed using a B3LYP functional and a LACVP** basis set with a Poisson-Boltzmann (PBF) CH_2Cl_2 solvent dielectric continuum as implemented in Jaguar.

Acknowledgements: The authors thank Professor Travis Williams for stimulating discussions and support with VT NMR; Professor Ralf Haiges for support with single crystal X-ray crystallography. The research described here was carried out with the support of the Universal Display Corporation. The X-ray diffractometer is sponsored by National Science Foundation CRIF Grant 1048807.

Notes and references

[a] *Department of Chemistry, University of Southern California, Los Angeles, California 90089, United States*

[b] *School of Pharmaceutical Science and Technology, Tianjin University, 92 Weijin Road, Nankai District, Tianjin, 300072, P. R. China*

† Electronic supplementary information (ESI) available: **:** ^{1}H NMR, gCOSY, 1-D NOESY, ^{13}C NMR, VT NMR of (corpy)Pt(dpm) and (phenpy)Ir(ppz)$_2$, Eyring analysis, CV of the complexes and emission spectra of the free corpy and phenpy ligand. For ESI and crystallographic data in CIF or other electronic format see DOI:

1. H. W. Kroto, J. R. Heath, S. C. Obrien, R. F. Curl and R. E. Smalley, *Nature*, 1985, **318**, 162-163.

2. F. Diederich and M. Gomez-Lopez, *Chemical Society Reviews*, 1999, **28**, 263-277.

3. R. Taylor and D. R. M. Walton, *Nature*, 1993, **363**, 685-693.

4. M. Prato, *Journal of Materials Chemistry*, 1997, **7**, 1097-1109.

5. P. W. Rabideau and A. Sygula, *Accounts of Chemical Research*, 1996, **29**, 235-242.

6. L. T. Scott, *Pure and Applied Chemistry*, 1996, **68**, 291-300.

7. Y.-T. Wu and J. S. Siegel, *Chemical Reviews*, 2006, **106**, 4843-4867.

8. B. M. Wong, *Journal of Computational Chemistry*, 2009, **30**, 51-56.

9. S. Sanyal, A. K. Manna and S. K. Pati, *Chemphyschem*, 2014, **15**, 885-893.

10. K. Shi, T. Lei, X.-Y. Wang, J.-Y. Wang and J. Pei, *Chemical Science*, 2014, **5**, 1041-1045.

11. L. T. Scott, M. M. Hashemi and M. S. Bratcher, *Journal of the American Chemical Society*, 1992, **114**, 1920-1921.

12. T. J. Seiders, K. K. Baldridge, J. M. Oconnor and J. S. Siegel, *Journal of the American Chemical Society*, 1997, **119**, 4781-4782.

13. T. J. Seiders, K. K. Baldridge, G. H. Grube and J. S. Siegel, *Journal of the American Chemical Society*, 2001, **123**, 517-525.

14. U. D. Priyakumar and G. N. Sastry, *Journal of Organic Chemistry*, 2001, **66**, 6523-6530.

15. P. A. Vecchi, C. M. Alvarez, A. Ellern, R. J. Angelici, A. Sygula, R. Sygula and P. W. Rabideau, *Organometallics*, 2005, **24**, 4543-4552.

16. S. Nishida, Y. Morita, A. Ueda, T. Kobayashi, K. Fukui, K. Ogasawara, K. Sato, T. Takui and K. Nakasuji, *Journal of the American Chemical Society*, 2008, **130**, 14954-+.

17. J. Brooks, Y. Babayan, S. Lamansky, P. I. Djurovich, I. Tsyba, R. Bau and M. E. Thompson, *Inorganic Chemistry*, 2002, **41**, 3055-3066.

18. A. B. Tamayo, B. D. Alleyne, P. I. Djurovich, S. Lamansky, I. Tsyba, N. N. Ho, R. Bau and M. E. Thompson, *Journal of the American Chemical Society*, 2003, **125**, 7377-7387.

19. J. Li, P. I. Djurovich, B. D. Alleyne, M. Yousufuddin, N. N. Ho, J. C. Thomas, J. C. Peters, R. Bau and M. E. Thompson, *Inorg. Chem.*, 2005, **44**, 1713-1727.

20. A. Bossi, A. F. Rausch, M. J. Leitl, R. Czerwieniec, M. T. Whited, P. I. Djurovich, H. Yersin and M. E. Thompson, *Inorganic Chemistry*, 2013, **52**, 12403-12415.

21. T. Sajoto, P. I. Djurovich, A. B. Tamayo, J. Oxgaard, W. A. Goddard, III and M. E. Thompson, *Journal of the American Chemical Society*, 2009, **131**, 9813-9822.

22. H. Yersin, A. F. Rausch, R. Czerwieniec, T. Hofbeck and T. Fischer, *Coordination Chemistry Reviews*, 2011, **255**, 2622-2652.

23. P.-T. Chou and Y. Chi, *Chemistry-a European Journal*, 2007, **13**, 380-395.

24. T. Sajoto, P. I. Djurovich, A. Tamayo, M. Yousufuddin, R. Bau, M. E. Thompson, R. J. Holmes and S. R. Forrest, *Inorg. Chem.*, 2005, **44**, 7992-8003.

25. Y. You and S. Y. Park, *Dalton Transactions*, 2009, 1267-1282.

26. L. Flamigni, A. Barbieri, C. Sabatini, B. Ventura and F. Barigelletti, *Photochemistry and Photophysics of Coordination Compounds Ii*, 2007, **281**, 143-203.

27. M. Yamada, S. Tashiro, R. Miyake and M. Shionoya, *Dalton Transactions*, 2013, **42**, 3300-3303.

28. R. Tsuruoka, S. Higashibayashi, T. Ishikawa, S. Toyota and H. Sakurai, *Chemistry Letters*, 2010, **39**, 646-647.

29. C. Thilgen and F. Diederich, *Chemical Reviews*, 2006, **106**, 5049-5135.

30. B. Ma, P. I. Djurovich, M. Yousufuddin, R. Bau and M. E. Thompson, *J. Phys. Chem. C*, 2008, **112**, 8022-8031.

31. M. Ghedini, D. Pucci, A. Crispini and G. Barberio, *Organometallics*, 1999, **18**, 2116-2124.

32. J. C. Hanson and C. E. Nordman, *Acta Crystallographica Section B-Structural Science*, 1976, **32**, 1147-1153.

33. A. S. Filatov, L. T. Scott and M. A. Petrukhina, *Crystal Growth & Design*, 2010, **10**, 4607-4621.

34. G. L. Miessler and D. A. Tarr, *Inorganic chemistry*, Pearson Education, Upper Saddle River, N.J., 2004.

35. F. J. Lovas, R. J. McMahon, J. U. Grabow, M. Schnell, J. Mack, L. T. Scott and R. L. Kuczkowski, *Journal of the American Chemical Society*, 2005, **127**, 4345-4349.

36. P. M. Morse, M. D. Spencer, S. R. Wilson and G. S. Girolami, *Organometallics*, 1994, **13**, 1646-1655.

37. K. Dedeian, J. M. Shi, N. Shepherd, E. Forsythe and D. C. Morton, *Inorganic Chemistry*, 2005, **44**, 4445-4447.

38. P. J. Hay, *Journal Of Physical Chemistry A*, 2002, **106**, 1634-1641.

39. C. Bruno, R. Benassi, A. Passalacqua, F. Paolucci, C. Fontanesi, M. Marcaccio, E. A. Jackson and L. T. Scott, *Journal of Physical Chemistry B*, 2009, **113**, 1954-1962.

40. K. Meerholz and J. Heinze, *Journal of the American Chemical Society*, 1989, **111**, 2325-2326.

41. N. M. Shavaleev, F. Monti, R. Scopelliti, A. Baschieri, L. Sambri, N. Armaroli, M. Graetzel and M. K. Nazeeruddin, *Organometallics*, 2013, **32**, 460-467.

42. A. Endo, K. Suzuki, T. Yoshihara, S. Tobita, M. Yahiro and C. Adachi, *Chemical Physics Letters*, 2008, **460**, 155-157.

43. A. Ito and T. J. Meyer, *Physical Chemistry Chemical Physics*, 2012, **14**, 13731-13745.

44. A. Ito, T. E. Knight, D. J. Stewart, M. K. Brennaman and T. J. Meyer, *The Journal of Physical Chemistry A*, 2014.

45. R. Englman and J. Jortner, *Molecular Physics*, 1970, **18**, 145-&.

46. H. Yersin, *Highly Efficient OLEDs with Phosphorescent Materials*, Wiley- VCH, Weinheim, 2008.

47. P. Y. Chen and T. J. Meyer, *Chemical Reviews*, 1998, **98**, 1439-1477.

48. M. Nonoyama, *Bulletin of the Chemical Society of Japan*, 1974, **47**, 767-768.

49. A. M. Butterfield, B. Gilomen and J. S. Siegel, *Organic Process Research & Development*, 2012, **16**, 664-676.

50. O. Lohse, P. Thevenin and E. Waldvogel, *Synlett*, 1999, 45-48.

51. R. R. Gagne, C. A. Koval and G. C. Lisensky, *Inorganic Chemistry*, 1980, **19**, 2854-2855.

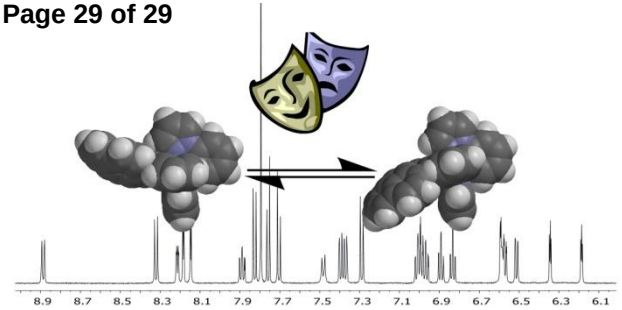

Novel, emissive Pt(II) and Ir(III) complexes are the first to have measured rates of inversion of cyclometalated corannulene.